Theor. Appl. Climatol. 73, 53–65 (2002)
DOI 10.1007/s00704-002-0693-5

Theoretical and Applied Climatology
Printed in Austria

[1] Meteorological Observatory Lindenberg, German Meteorological Service (DWD), Lindenberg, Germany
[2] Aerospace Systems, Technical University of Braunschweig, Braunschweig, Germany

Determination of boundary-layer parameters using wind profiler/RASS and sodar/RASS in the frame of the LITFASS project

D. A. M. Engelbart[1] and **J. Bange**[2]

With 5 Figures

Received June 16, 2001; revised February 20, 2002; accepted May 30, 2002
Published online November 19, 2002

Summary

Progress in technology as well as signal processing has promoted *W*ind *P*rofiler *R*adar (WPR) or sodar with RASS additions to become standard tools in profiling of the atmospheric boundary layer. Apart from these instruments' basic abilities in profiling mean winds and temperature, this paper will give an emphasis on the profiling of ABL height as well as the turbulent fluxes of sensible heat and momentum both, with respect to methods as well as with respect to realization. The special focus will thereby be laid on the demands for vertical profiling, which were defined within the LITFASS-project of the German Meteorological Service. In the frame of this project, some special measuring campaigns have been performed where remote-sensing systems were used to assess their abilities in profiling ABL parameters. On the base of some case studies from these campaigns comparisons are shown, where results from sodar/RASS and WPR/RASS measurements are compared to measurements from airborne sensor systems and results from numerical models. Regarding turbulent heat fluxes, we found excellent agreement for remotely-sensed flux profiles from WPR/RASS with both, numerical models and airborne in-situ measurements. However, as the inherent errors of the remotely-sensed fluxes are in the order of $\pm 20 \cdots 30\,\mathrm{W/m^2}$ typically, current signal processing does not allow to interpret small-scale vertical structures in the profiles with respect to surface inhomogeneities yet.

1. Introduction

The LITFASS-project of the German Meteorological Service (DWD) (Müller et al., 1995) generally focused interest on an experimental determination but also on numerical modelling and parameterization respectively of the spatially averaged turbulent fluxes of heat (latent and sensible) and momentum over an inhomogeneous meso-γ scale terrain.

Within the general strategy of the LITFASS-project (see Beyrich et al., 2002), the objectives for remote profiling of atmospheric boundary layer ABL parameters were not only focussed onto basic research but on the operational user's needs. These needs were particularly connected to the following demands:

- Supply of (mean) assimilation data for numerical modeling (wind, temperature, humidity/water vapour),
- supply of mean profiling data and turbulence parameters for validation of numerical model output, and
- test of new profiling algorithms and parameterization results by use of high-resolution model output.

Coming from these demands for remote profiling of the ABL, this paper will demonstrate the up-to-date abilities of measuring different kinds of boundary-layer parameters using acoustic and electromagnetic remote-sensing tools such as sodar and *W*ind *P*rofiler *R*adar (WPR) in combination with "*R*adio-*A*coustic *S*ounding *S*ystems" (RASS). While the different techniques of remote profiling using sodar, WPR as well as both types of RASS, i.e. Bragg-RASS and Doppler-RASS are described elsewhere (e.g. Weill, 1986; Doviak and Zrnic, 1993) and detailed descriptions on the WPR/RASS and sodar/RASS used in the frame of the present study are depicted in Engelbart et al. (1996), Steinhagen et al. (1998), and Engelbart et al. (1999), the particular interest will here be laid on the determination of boundary-layer heights as well as profiles of turbulent fluxes, where especially evaluations of case studies during the LITFASS-project will be shown in order to demonstrate the potential of the different methods proposed for being employed with active remote-sensing techniques. In addition to the simple application of different methods, this paper will furthermore give an impression on the quality of the derived quantities by means of comparisons with a number of validation systems and techniques for independent comparison.

2. Boundary-layer height

Monitoring the boundary-layer height z_i and its evolution in time has been of major interest for ground-based remote sensing from the very beginning. Generally, there are two basic ABL regimes which can be distinguished according to the dominant production mechanism of turbulence, i.e. the stably-stratified and the convective boundary layer. Corresponding to their range and vertical resolution, sodars have mainly been used to study the internal structure of the stably-stratified boundary layer and the transition of the ABL from stable to unstable. It has also been a major objective in the past, trying to get the height of the boundary layer and its diurnal variations from sodar measurements. However, due to the range restrictions of sodars, these attempts had to make use of some parameterizations or have to be supplemented by numerical models. A summary of these attempts as well as a technique using the latter approach is given e.g. by Beyrich (1997).

A different tool, not suffering in range restrictions with respect to the daytime boundary-layer height, is the WPR technique. Hence, WPR are used increasingly in order to study the height of the convective boundary layer, also known as mixed-layer (ML) depth (Stull, 1988) or mixing height (COST-710, 1998), and the entrainment zone, i.e. roughly the vertical range of the ABL-capping inversion. On the other hand, WPR typically are restricted to measurements above about 100–300 m in height, whereas this range of heights fairly often defines the depth of nighttime boundary layers. Thus, WPR are not well suited for monitoring nighttime conditions and nighttime variations of the boundary-layer height.

To get rid of the single-system dilemma, the optimal solution would therefore be a combination of sodar and WPR (e.g. Beyrich and Görsdorf, 1995), particularly if both are combined with RASS. Throughout the LITFASS-project, the method of combining both instruments in order to get a complete diurnal cycle of the ABL height has been tested as well as verified during some special field campaigns. Results from these evaluations will be shown in the following subsections.

2.1 Convective boundary layers

For a determination of the mixing height, describing the depth of a convective boundary layer, in principle two different approaches from WPR/RASS measurements and WPR respectively may be applied. The first approach which simply uses the standard evaluation known from radiosoundings, makes use of the vertical profile of virtual temperature from WPR/RASS. Applying a temperature criterion,

$$z_i = z_0 + \frac{\Delta E_z}{2},$$

for determination of the mixing height z_i (e.g. Stull, 1988), RASS temperature measurements can be used for evaluation of the height range ΔE_z of the first free inversion above surface, which roughly equals the depth of the entrainment zone, and whose lower border is described

by z_0. This method works fairly well as long as the range of ΔE_z is not too small compared to the range resolution of the WPR/RASS, and as long as the convective boundary layer is really well mixed below the inversion and $d\theta(z)/dz = 0$, where θ defines potential temperature. Furthermore, a problem concerning RASS data evaluations is connected to the restricted vertical range of acoustic remote sensing. Using a high-UHF WPR, which has to use the 1290 MHz frequency in Germany, the corresponding ≈ 3 kHz of the acoustic RASS signal only covers a height range of about 1 km maximum. Hence, using RASS is not suitable to monitor mixing heights under strongly convective and summertime conditions, especially.

Apart from using RASS and the temperature profile for monitoring mixing height, a second method may be applied using pure WPR data. This method does not show the disadvantage of RASS with respect to range but makes use of the connection between Radar return-signal power and temperature gradient. The background is that backscattered signal power or radar reflectivity η under conditions of pure clear-air scattering (Bragg scattering) is proportional to the squared refractive index structure constant C_n^2 (e.g. Ottersten, 1969a), i.e.,

$$\eta \simeq 0.38\, C_n^2\, \lambda^{-1/3}, \tag{1}$$

and C_n^2 on the other hand, is strongly depending on fluctuations of humidity and temperature. As both temperature and humidity fluctuations above the surface layer should show a relative maximum in the height range of free inversions, the entrainment zone and therefore the mixing height should be detectable, because convective boundary layers do not show intermediate structures ideally, with respect to temperature within the mixed layer.

2.2 Stably-stratified boundary layers

Since stably-stratified (nocturnal) boundary layers typically extend only up to 100–300 m in height, WPR systems as well as RASS additions to them show two fundamental disadvantages: These are at first the lower boundary of the measuring range of RASS temperatures, which is about 250 m in height above ground level for the 1290 MHz WPR/RASS of the German Meteorological Service (DWD) at the Meteorological Observatory Lindenberg (MOL) (Engelbart et al., 1996). Therefore, the first range gate frequently starts above the nocturnal boundary layer. A second disadvantage is defined by the gate spacing of the WPR/RASS. In common systems, this resolution is between 45 m and 60 m or frequently 100 m. Both of these disadvantages can be avoided using a sodar system in combination with a Doppler RASS. For the sodar/RASS at MOL (Engelbart et al., 1999) the first range gate starts at 10 m or 20 m (RASS), having a minimum gate spacing of 5 m.

A common diagnostic method, being applied frequently in numerical simulation models for determination of the depth of the stably-stratified, nocturnal boundary layer, uses vertical profiles of the bulk Richardson number (e.g. Fay et al., 1997). This approach, which is numerically robust and fairly accurate according to Vogelezang and Holtslag (1996) and therefore more suitable than a pure temperature criterion, is also highly suited for evaluations of sodar data, as far as the sodar-derived vertical profiles of wind are supplemented by quasi-simultaneous measurements of virtual temperatures using RASS. An impression on this possibility for the derivation of the nocturnal ABL depth is demonstrated in Fig. 1. The data of this figure are based on measurements at 17 May, 1998 using the Metek *DSDPA.90* sodar/RASS at the MOL (Engelbart et al., 1999) with an acoustic frequency of 1675 Hz, a vertical resolution of $\Delta z = 20$ m and an averaging time interval of $\Delta t = 15$ min. Concerning sensitivity of the results, the value chosen for the critical Richardson number, $\mathrm{Ri_c} = 0.35$, defining the top of the boundary layer within the vertical profile of Ri (Soerensen et al., 1997), seems to be insensitive in a range between 0.28 and 0.40. Generally, the time series of the depth of the nocturnal boundary layer shows reasonable results for this case study. It therefore demonstrates the applicability of the Richardson number approach for the derivation of stably-stratified (nocturnal) boundary-layer depths from sodar/RASS data.

2.3 Case studies and validation

In order to avoid the range restriction of sodars, the use of WPR or a combination of sodar and

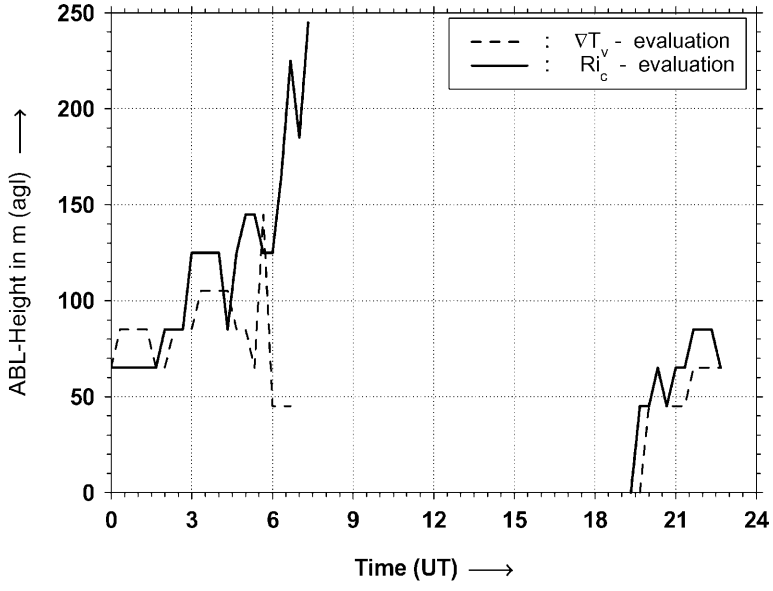

Fig. 1. Height of the stable (nocturnal) boundary layer at 17 May, 1998, derived from sodar/RASS using a Richardson-number criterion with $Ri_c = 0.35$ (solid) and derived from max (θ) (dashed)

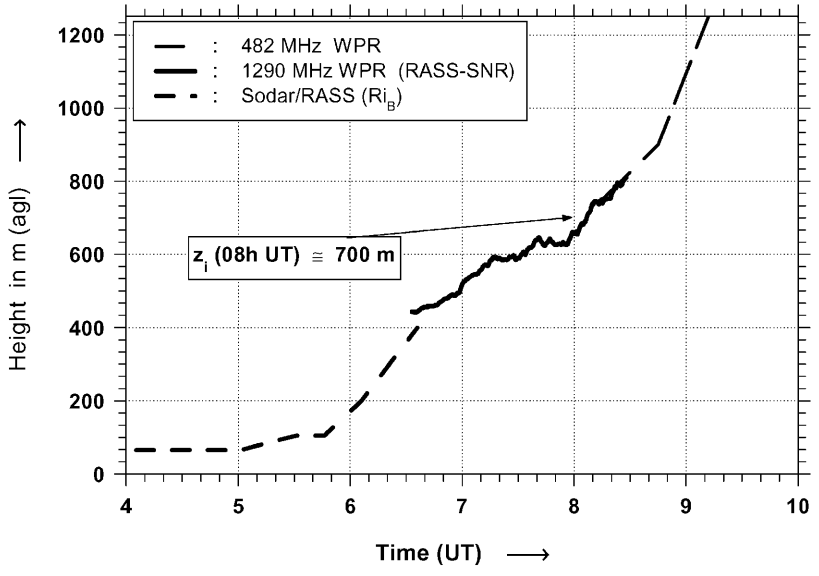

Fig. 2. ABL height on 18 June, 1998, 4:00 h–10:00 h UT, as derived from three different remote-sensing systems (see text)

WPR is favourable. The advantageous combination of WPR and RASS is shown in a case study which refers to 18 June, 1998. At this day, additional measurements, i.e. aircraft- and helicopter-based sensors were available apart from sodar/RASS and WPR/RASS evaluations (see also: Bange et al., 2002). As the 1290 MHz WPR/RASS was used primarily for measuring vertical profiles of the turbulent heat flux, its vertical range was restricted to about 800 m at this day. Hence, a second WPR/RASS (TWP), using 482 MHz frequency and having a coarser vertical spacing (Steinhagen et al., 1998) was used to supplement the time series of the ML depth. Figure 2 reveals the time series of the ABL depth for this day from both sodar/RASS and the two different WPR systems, where the sodar/RASS data have been evaluated with respect to the profile of the bulk Richardson number and the WPR data with respect to radar reflectivity.

Due to the restricted height range of the sodar/RASS but also of the 1290 MHz WPR, these systems were not able to supply the full time series until 10 h UT. For the 1290 MHz system, this came into effect after about 08 h UT. However, due to the additional measurements of the 482 MHz system, being located just 50 m beside the 1290 MHz system, an uninterrupted

time series could nevertheless be provided for the intended period of time between 07:30 h and 08:30 h UT. Apart from this paper, the resulting time series from a composite profiling of the mixing height by sodar/RASS and two WPR systems is confirmed also by some airborne systems as shown by Bange et al. (2002).

In conclusion, this example of determining ABL depths particularly shows the advantages of combined systems, because not only sodar/RASS but also WPR/RASS is affected by range restrictions throughout the day, typically. Combinations of these systems could therefore be a means to avoid these kind of problems. For the operational and unattended monitoring of the ABL depth however, additional systems (e.g. a cloud radar) have to be added which provide information on the prerequisite of pure clear-air scattering.

In addition to single case studies, also a long-term comparison between WPR/RASS-derived ABL heights and results from a numerical model (''DM'') have been performed during the LITFASS-project. Although WPR/RASS-derived heights generally show a reasonable agreement with results from the numerical model, which uses a Richardson-number criterion for determination of the ABL depth (Fay et al., 1997), the model typically underestimates the daytime mixed-layer maximum slightly. However, large differences of more than 300 m, were generally caused by forecast errors of the numerical model.

3. Vertical profiles of the turbulent fluxes of heat and momentum

For the closure of the prognostic equations of the ABL either experimental data on turbulent fluxes of momentum, sensible heat, and latent heat or those from numerical model runs are needed. This is connected to the fact that the ABL always reflects features of the usually non-homogeneous conditions at the surface. Therefore, the challenge is not only to know the surface-layer values of turbulent fluxes, but their vertical profiles.

While ABL heights or mean vertical profiles, i.e. zero- or first-order quantities may be measured comparably easy, a determination of second-order moments like fluxes or variances are much more difficult. Hence, many efforts have been made in the past to derive the latter from remote-sensing data as these show significant advantages with respect to time resolution compared to classical balloon-borne systems.

Apart from measuring, on the other hand, many years and efforts have been spent in the past to create simple models of the vertical profile of fluxes in the ABL. These models are based on the surface values of fluxes and some information on the type of stratification of the ABL. However, the peculiarities of the vertical structure of the ABL due to e.g. surface inhomogeneities, meso- and micro-scale flows, air-mass advection etc. defy modeling. Vice versa it is also fairly difficult to verify or validate results of a numerical model by measured ''truth''. In this respect, the most suitable tools to attain progress in measuring full-ABL profiles of turbulent fluxes reliably is ground-based remote sensing using sodar, WPR, or lidar systems.

The application of remote-sensing systems for determination of second-order moments has started in the early eighties, when sodar was used for measuring vertical velocity variances. Recent studies in this field have been published e.g. by Peters et al. (1998), who compared sodar-derived variances with data from ultrasonic anemometers. WPRs have been used commonly in various boundary-layer field campaigns since the eighties. First studies here were published e.g. by Peters et al. (1985) or Angevine et al. (1993, 1994). More recent investigations are focussing now interest e.g. on comparisons with direct measurements (e.g. Engelbart and Klein Baltink, 1997; Engelbart, 1998; Potvin et al., 1998) or on a determination of the entrainment-zone thickness using WPR and lidar (Cohn and Angevine, 2000).

Finally, also lidars have been used either standalone, e.g. to measure profiles of the water vapour variance or in combination with WPR in order to get profiles of the latent heat flux (e.g. Senff et al., 1994; Wulfmeyer and Böesenberg, 1998; Wulfmeyer, 1999).

Within the LITFASS-project, one of the major objectives with respect to remote sensing has been the measurement of vertical profiles of the turbulent flux of sensible heat by WPR/RASS and its interpretation with respect to inhomogeneities of the surrounding land surface (Engelbart, 1998).

3.1 Theoretical background

3.1.1 Basic equations for the vertical turbulent heat flux (buoyancy flux)

Generally, the vertical turbulent flux of sensible heat H is defined by the covariance of vertical wind speed w and potential temperature θ, i.e.,

$$H = \varrho \cdot c_p \cdot \overline{w'\theta'}, \tag{2}$$

where ϱ denotes the density of air, c_p the specific heat of air at constant pressure, and the primed quantities indicate deviations from mean values according to the perturbation approach. Applying (2) to measurements is called the *eddy-correlation* technique.

RASS temperatures generally base on measurements of the acoustic propagation velocity c_R (RASS velocity). In the atmosphere, this propagation is influenced by air motion, i.e. wind speed. In case of a vertically-pointing RASS, acoustic propagation therefore rewrites to

$$c_R = c_a(T_v) + w,$$

with the speed of sound $c_a = c_a(T_v)$ and w as vertical wind speed. By decomposition of c_R as well as vertical wind speed into mean value and perturbation again, and by subsequent rearrangement of the terms according to the definition of the covariance $\overline{w'\theta'_v}$ we yield

$$\begin{aligned}\overline{w'\,\theta'_v} &= \frac{\alpha\,(N-1)}{2\,N} \cdot \left(\sigma^2_{c_R} - \frac{1}{\alpha^2}\,\sigma^2_{\theta_v} - \sigma^2_w\right) \\ &\simeq \frac{\alpha}{2} \cdot \left(\sigma^2_{c_R} - \frac{1}{\alpha^2}\,\sigma^2_{\theta_v} - \sigma^2_w\right),\end{aligned} \tag{3}$$

where

$$\alpha = 2 \cdot \sqrt{\frac{\theta_v}{\gamma\,R_a}}, \tag{4}$$

γ describes the ratio of specific heats, and R_a is the gas constant of air. Using (4) Eq. (3) now mainly consists of the three variances $\sigma^2_{c_R}, \sigma^2_{\theta_v}$, and σ^2_w. These quantities can either be measured directly or parameterized as well. Because $\frac{1}{\alpha^2}\,\sigma^2_{\theta_v}$ is significantly smaller than the other variances and therefore much more sensitive to measuring errors than these, it could either be neglected or parameterized as well. In case of a convective boundary layer such a parameterization might be (Stull, 1988)

$$\sigma^2_{\theta_v}(\text{convective}) = T^2_{*,ML} \cdot 1.8 \cdot \left(\frac{z}{z_i}\right)^{-2/3}. \tag{5}$$

In this equation, the mixed-layer temperature scale is defined as

$$T^2_{*,ML} = \left(\frac{w^2_* \theta_v}{g\,z_i}\right)^2, \tag{6}$$

and the Deardorff velocity for the mixed layer, w_*, writes

$$w_* = \left[\frac{\sigma^2_w}{1.8\,\left(\frac{z}{z_i}\right)^{2/3} \cdot \left(1 - 0.8\,\frac{z}{z_i}\right)^2}\right]^{1/2}, \tag{7}$$

when defined by means of $\sigma^2_w = f\left(\frac{z}{z_i}\right)$.

From these relations, i.e. by substituting (7) into (6) and application of the resulting equation in (5), the variance of potential temperature $\sigma^2_{\theta_v}$ is derived roughly.

3.1.2 Basic equations for the vertical turbulent flux of momentum

In analogy to the derivation of the variance method for heat fluxes from remote-sensing data, also relations for determination of momentum-flux profiles may be derived. Coming from the decomposition for the radial velocity in direction of (e.g.) the u component of wind velocity, $v_{r_u} = u\sin\phi + w\cos\phi$, where the angle ϕ represents distance from zenith, and after application of the variance operator we reach at the following relations,

$$\overline{w'u'} = \frac{N-1}{2N\cos\phi\sin\phi} \cdot (\sigma^2_{v_{ru}} - \sigma^2_u \sin^2\phi - \sigma^2_w \cos^2\phi), \tag{8}$$

for the flux component in the direction of u and

$$\overline{w'v'} = \frac{N-1}{2N\cos\phi\sin\phi} \cdot (\sigma^2_{v_{rv}} - \sigma^2_v \sin^2\phi - \sigma^2_w \cos^2\phi), \tag{9}$$

for the component in the direction of v, where the total flux τ calculates from

$$\begin{aligned}\tau &= +\varrho \cdot \overline{w'v'_h} = +\varrho \cdot \sqrt{\overline{w'u'}^2 + \overline{w'v'}^2} \\ &= -\varrho \cdot u^2_*.\end{aligned} \tag{10}$$

These equations can be used directly for application to 3-beam configurations of WPR or sodar systems. However, at the cost of one or two more beams, i.e. of some loss of time resolution, it is easier to use a four- or five-beam configuration utilizing pairs of opposite beams in the same plane. Having these data, e.g., for the

u component $v_{r_{u+}} = +u \cdot \sin\phi + w \cdot \cos\phi$ and $v_{r_{u-}} = -u \cdot \sin\phi + w \cdot \cos\phi$ and similarly for the v component, the flux reduces to the relation according to Peters and Kirtzel (1994)

$$\overline{w'u'} = \frac{\sigma^2_{v_{r_{u+}}} - \sigma^2_{v_{r_{u-}}}}{4 \cdot \sin\phi \cdot \cos\phi}. \tag{11}$$

These easy relations are most promising as long as time resolution is good enough for covering the inertial subrange of turbulence or at least the bulk of energy-carrying eddies. However, for the (e.g.) 1290 MHz WPR/RASS at MOL the necessary time for an acceptable compromise between data quality and time resolution is about 25 s per beam, i.e. the time needed for getting instantaneous values of τ is about 2 min for a five-beam configuration. As this is too coarse for the height range of interest, either different techniques (e.g. spaced-antenna methods) or parameterizations have to be used in order to get vertical profiles of the turbulent momentum flux.

3.2 Selected parameterizations for heat and momentum fluxes from WPR/RASS and SODAR/RASS

As an alternative to directly measuring turbulent fluxes and additionally for getting first qualitative impressions on measured data, some parameterizations have been used for application with sodar/RASS as well as WPR/RASS data. A simple first parameterization may be derived from thermodynamics.

Assuming advection-free conditions as well as negligible divergences of the radiation flux and dissipation, the first theorem of thermodynamics maybe reformulated to be

$$\frac{\partial\theta}{\partial t} \approx +\frac{\partial}{\partial z}\left(\frac{H}{\varrho c_p}\right). \tag{12}$$

When this equation is integrated between the surface layer and the height of the mixed layer, z_i, we receive

$$\int_0^{z_i} \frac{\partial\theta}{\partial t} dz = \frac{1}{\varrho c_p} \int_0^{z_i} dH = \frac{1}{\varrho c_p}(H_i - H_0). \tag{13}$$

With the assumption of a fixed relationship $H_i = -aH_0$ (e.g. Arya, 2001) for the heat flux between mixing height $H(z_i)$ and that of the surface layer H_0, where the factor $a = 0.2$ maybe received e.g. from Stull (1976), who summarized values for this parameter from 35 different articles, we finally reach at

$$H_0 = \frac{\varrho\, c_p\, z_i}{1.2} \cdot \frac{\Delta\theta}{\Delta t}. \tag{14}$$

Although this relation does not supply information on the effect of surface-layer inhomogeneities to the flux profile, it nevertheless already gives hints on the realism of the remotely-sensed heat flux profile.

Due to restrictions with time resolution when directly measuring momentum fluxes (see 3.1.2), and furthermore for avoiding conflicts with the need for switching to special measuring modes at WPR or sodar, one of the ideas regarding remote sensing in the frame of the LITFASS-project was to look for and to test parameterization schemes which are applicable to WPR/RASS and/or sodar, both in principle and particularly with respect to the routine mode's data of the systems. For being able to locate effects of surface inhomogeneities in vertical flux profiles, the nonlocal transilient turbulence parameterization (*TTP*) scheme (Stull, 1993) has been applied. Details on an application of this parameterization using sodar/RASS data will be given in the frame of a special publication. First results are already in Engelbart and Steinhagen (2001).

3.3 Error estimators for remotely-sensed fluxes and variances

In order to assess the quality of remotely-sensed heat fluxes, an estimation of possible errors has to be made. Concerning errors, the largest contribution for this kind of measurement is caused by the statistical behaviour of the atmosphere itself. This is described by the so-called sampling error, which is caused by the uncertainty of determining the ensemble average of a quantity by a limited number of measurements (sample). With respect to a profiling of sensible heat fluxes, this sampling error ΔH can be determined in agreement with Wyngaard (1992) and Lenschow et al. (1994) by

$$\Delta H = \varrho\, c_p \cdot \sqrt{\frac{2\sigma^2_{w'T'_v}\, \tau_{is}}{N\, \Delta t}}, \tag{15}$$

where the error of the ensemble, i.e. ΔH, is connected to the variance of the measured sample

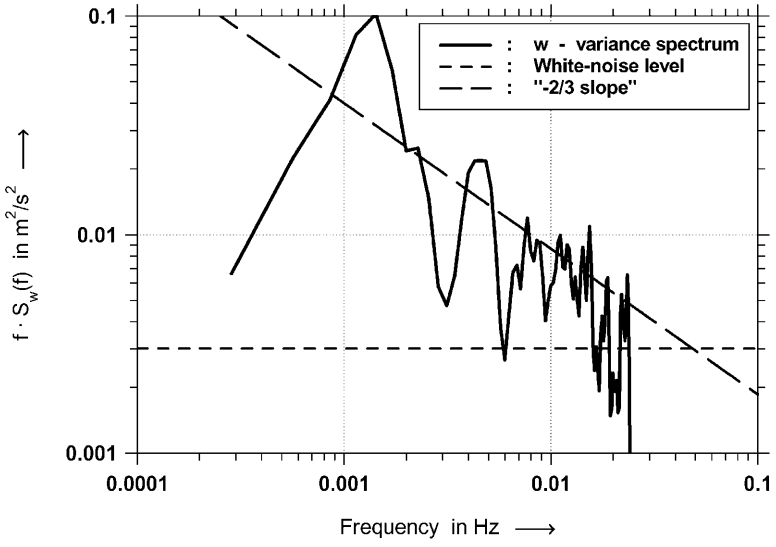

Fig. 3. Variance spectrum of the vertical velocity for 18 June, 1998, 08 h–09 h UT at a height range of 337 m. The inertial subrange portion of the spectrum should appear as a straight line with a $-2/3$ slope, as indicated by the dashed line. Additionally, the evaluation of the statistical (noise) error has been indicated by the horizontally-dashed line

(i.e. covariance) $\sigma^2_{w'T'_v}$ by an '*integral time scale*' τ_{is} and the averaging interval, represented by time resolution Δt of the measurements and number of samples N. In (15), according to Lenschow et al. (1994), τ_{is} is defined as

$$\tau_{is} = \int_0^\infty R_{w'T'_v}(t)/R_{w'T'_v}(0)\, dt, \tag{16}$$

which describes the integral time scale as a function of the ratio of autocovariances at dislocation t versus lag 0, which is the autocorrelation function $\varrho_{w'T'_v}(t)$ and which can easily be calculated from time series data. The only prerequisite for correctness of the sampling error now bases on the assumption that the samples of w and T_v are distributed Gaussian, as in this case it follows for the variance $\sigma^2_{w'T'_v}$ of the sample (Lenschow and Stankov, 1986)

$$\sigma^2_{w'T'_v} = \overline{w'^2}\;\overline{T'^2_v} + \overline{(w'T'_v)^2}. \tag{17}$$

In addition to the sampling error according to Wyngaard (1992), Lenschow and Stankov (1986), and Lenschow et al. (1994) a second error, the noise error can be determined. The background for its determination, which has first been applied by Senff et al. (1994), is that noise, generated by statistically independent vertical velocity measurements is white. Therefore, the value at the high frequency end of the variance spectrum gives an estimation of the statistical (noise) error for the measured w-values. This measure gives an upper limit of the statistical error because atmospheric variations can still be included in the variance spectrum at the high frequency end. Doing evaluations of this error for variances of radial velocities however, it turns out that its influence is small compared with the sampling error above (see Fig. 3).

3.4 Case studies from the Litfass campaigns

According to the above mentioned relations for determination of turbulent fluxes, their application to sodar/RASS or WPR data seems to be fairly easy. However, problems grow with more detailed analyses, due to several reasons: Intending to apply eddy-correlation, the most obvious problems are:

- The occurrence of outliers mostly by intermittent clutter, i.e., by erroneous evaluation of hard targets instead of the clear-air return,
- the existence of return signals from ground clutter, i.e., fixed-echo targets indicating a zero radial velocity,
- the height-depending behaviour of data quality from WPR and sodar, due to the increasing number of outliers with height,
- the limited time resolution of radial velocity evaluations of about 25 s for WPR, and
- the coarse velocity resolution of the signal processing, resulting in highly noisy sampling of small-amplitude fluctuations in radial velocities, particularly in RASS mode.

In order to minimize the effect from problems like these, the following steps for WPR/RASS data have turned out to be optimal for data

conditioning. However, these steps only refer to eddy-correlation measurements of the virtual heat flux using WPR/RASS, as sodar/RASS data evaluation applying eddy correlation was not successful with respect to the necessary data quality. In this respect, there still is a major need for future investigations.

Prior to any data conditioning, the total time series is splitted into segments of 60 min duration for the subsequent data processing steps. This is in accordance with earlier investigations (Angevine et al., 1993a, b, 1998; Engelbart and Klein Baltink, 1997; Hirsch and Peters, 1998; Potvin et al., 1998). It furthermore agrees with evaluations of the cumulative integral of 4-hour averaged co-spectra of vertical velocity w and temperature T_v, indicating that $\geq 98\%$ of the total covariance will be covered, when evaluations are performed to 60 min time series in a height range up to the about 800 m.

The first step in data conditioning which is in agreement with Angevine et al. (1993a, b), then applies a statistical filter, in order remove far outliers from the original time series data. This filter uses a 2σ-criterion for detection. Secondly, data are being smoothed by an median filter similar to Potvin et al. (1998). However, while these authors use a simple dual-mode filter, i.e. low smoothing for the lower height range and strong smoothing for the upper range gates, the median filter applied here is linearly increasing from a width of 3 time steps at the lowest measuring height of about 300 m agl up to 31 steps at the uppermost height (typically about 800–900 m agl), i.e. it increases by 2 steps per height range taking into account the continuous decrease of data quality as well as the increasing potential size of turbulent eddies with height. Finally, the last step in data conditioning refers to the need of stationary time series. Thus, in order to eliminate the long-term non-turbulent behaviour of the measured time series, a linear trend elimination is applied.

Although the different steps of data conditioning usually prepare the 60 min segments of the WPR/RASS raw data highly effective for application of the eddy-correlation technique, which is either the covariance method according to (2) or the variance method (3), the method does not necessarily work at every 60 min segment. This problem occurs fairly often and is another reason for looking for some robust parameterization, in order to satisfy the needs of operational users. Generally, from the current status of investigations it seems obvious, that there is a kind of threshold density of erroneous data within the time series, when the eddy correlation starts to fail. However, its exact value has still to be investigated. It has furthermore to be mentioned that the necessary strength of Median filtering should be site-specific and adapted to the WPR system as well as to the surrounding situation of ground- and intermittent-clutter influence. In summary, the efforts in data conditioning must be performed with particular care in order to avoid negative influences onto the spectra of turbulence and the values of the resulting flux data subsequently.

An example for the quality of the high-resolution time-series data of WPR/RASS can be reached from evaluation of the statistical (noise) error of the vertical velocity according to 3.3. Figure 3 shows the variance spectrum of the vertical velocity w, referring to a height range of 337 m agl for 18 June, 1998. The ordinate of this figure represents the spectral variance density of the vertical velocity w, defined by

$$S_w(f) = \frac{2\,|F_w(f)|^2}{\Delta f} \tag{18}$$

and multiplied with frequency f. Here, $|F_w(f)|^2$ describes the squared sum of the real and imagery part of the Fourier transform, $F_w(f) = 1/T \int_0^T w(t) \cdot \exp^{-i\,2\pi ft}\,dt$. The total variance of the vertical velocity time series then results from

$$\sigma_w^2 = \int_f S_w(f)\,df. \tag{19}$$

The statistical noise error $S_{w,*}(f)$ according to Senff et al. (1994) is finally obtained by averaging the last 20% at the high frequency end of the 5-point moving-averaged spectrum, assuming white noise at this high-frequency end. Expressed in terms of a variance $\sigma_{w,*}^2$, this error is

$$\sigma_{w,*}^2 \simeq S_{w,*}(f) \cdot \left(f_N - \frac{1}{T_{tot}}\right), \tag{20}$$

where $f_N = 1/(2 \cdot \Delta t)$ denotes the Nyquist frequency (Δt = temporal resolution of the time series) and T_{tot} indicates the total length of the measurements with respect to time. Doing the above evaluation for the high resolution data of

18 June, 1998, 08–09 h UT, the resulting noise error e.g. for the height range $z = 337$ m is $\sigma_{w,*}(\mathrm{WPR}) \simeq 3\,\mathrm{cm/s}$.

In order to assess the absolute quality of remotely-sensed fluxes, different verifications apart from numerical model results have to be performed. For realization, two case studies from the LITFASS-98 pre-campaign in 1997 (14 June, 1997: 06:45 h–08:05 h UT) and from LITFASS-98 itself (18 June, 1998: 07:30 h–08:30 h UT) have therefore been chosen, where independent reference data from in-situ measuring systems were available. Details on the synoptic situation of 18 June, 1998 are described e.g., in Bange et al. (2002). Concerning the case study of the pre-campaign to LITFASS-98, the situation was highly instationary with some clouds above the CBL as well as rain starting after about 10 h UT. This instationarity is also reflected by the strong difference in the vertical profile of turbulent heat flux analyzed by the numerical model "DM4" for 07 h UT and 08 h UT. Results of these comparisons, where in-situ data, measured by the airborne sensor systems DO-128 and Helipod (see Bange et al., 2002) were available, are shown in Figs. 4 and 5.

In addition to the absolute reference represented by the airborne measuring systems, these figures furthermore show a comparison with results of numerical models. Concerning the data of the LITFASS-98 pre-campaign, again results from the DM4 are presented, whereas the evaluation for LITFASS-98 (see Fig. 5) also includes results from the micro-α scale model "LLM" (Herzog et al., 2002). The corresponding height of the ABL (mixing height) for both cases has been derived from WPR using the reflectivity method. The early-morning development of the mixing height at 18 June, 1998 derived from sodar and WPR (see Fig. 2) was shown above. Apart from this, a time series for the mixing height from WPR data at 18 June, 1998, as well as its verification compared to aircraft soundings is presented by Bange et al. (2002, Fig. 6).

Generally, both comparisons show good agreement between in-situ and remotely-sensed flux profiles and agree additionally well with numerical models. Furthermore, the variance and covariance methods applied to WPR/RASS, show reasonable agreement (Fig. 4). Figure 5 also reveals the effect of time averaging of the 10 min averaged data from the LLM. Looking again at

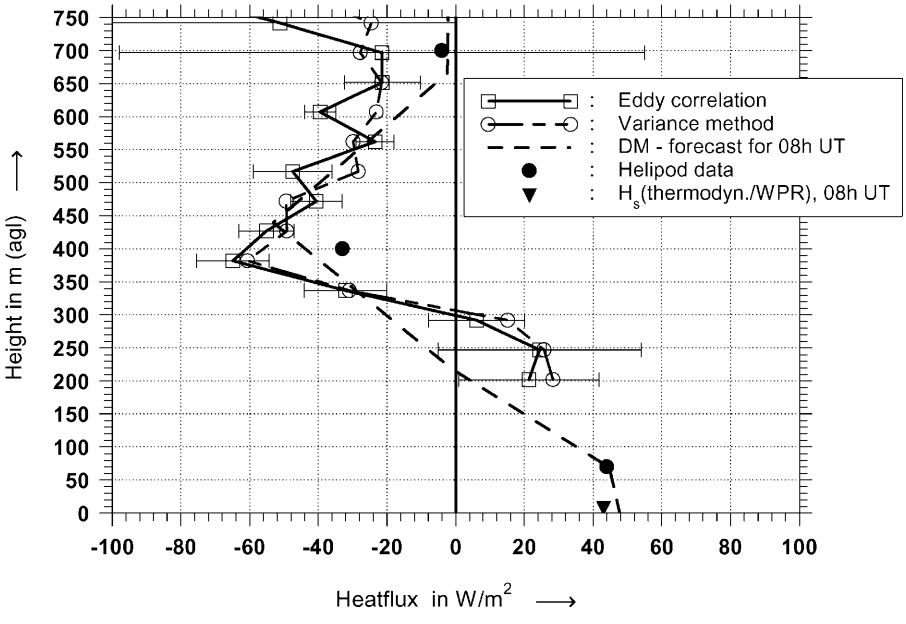

Fig. 4. Vertical profile of the virtual heat flux H (in $\mathrm{W/m^2}$) for 14 June, 1997, 06:45 h–08:05 h UT, as measured by the 1290 MHz WPR/RASS of the Meteorological Observatory Lindenberg during the LITFASS-98 pre-campaign in 1997. The graph is based on 25 s radial velocity data applied for the eddy correlation and variance technique in comparison to different validation data and methods. Error bars refer to the sampling error according to LS86. Heat fluxes from the Helipod system refer to the east leg of its flight schedule. For comparison, results from the numerical mesoscale model "DM4" of the DWD are shown

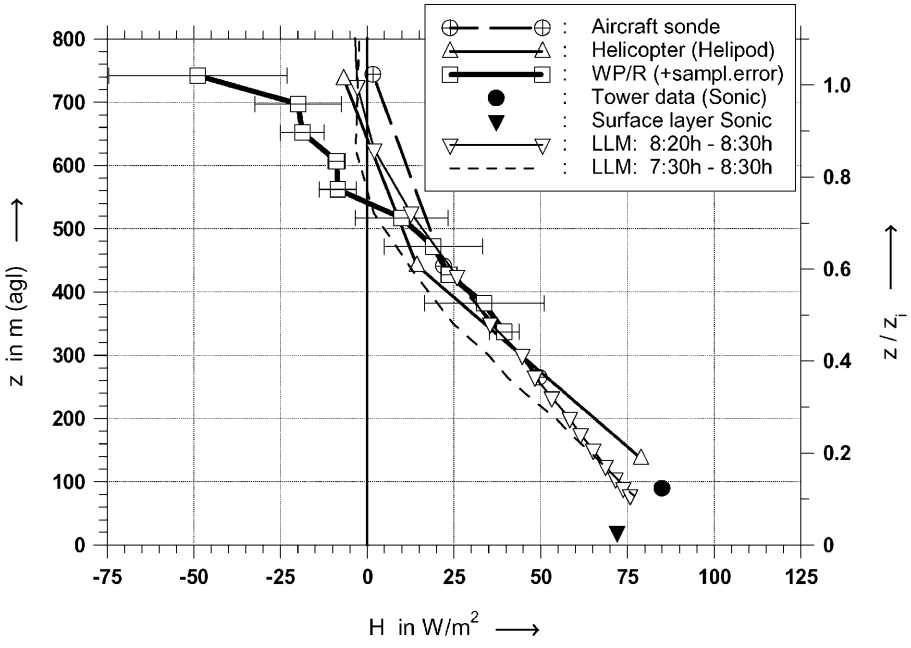

Fig. 5. Vertical profile of the virtual heat flux H (in W/m^2) for 18 June, 1998, 06:45 h–08:05 h UT, as measured by the 1290 MHz WPR/RASS of the Meteorological Observatory Lindenberg during the campaign of LITFASS-98. The graph is based on 25 s radial velocity data similar to Fig. 4 and compared to results of airborne measuring systems as well as the micro-α scale model "LLM"

the upper height range near the entrainment zone of the convective ABL at this day, the effect of sampling problems in combination with the increasing number of outliers at increasing heights becomes obvious. The absolute value of the sampling errors for the 1290 MHz WPR system furthermore indicates that the intended interpretation of vertical structures in the profile is only possible for very evident structures. Furthermore, it is expected that the altitude of the blending height (Claussen, 1991), indicating the upper limit of influence from surface inhomogeneities, usually is located below the minimum height range of the 1290 Mhz WPR/RASS. These problems have led to investigations on parameterizations for application with sodar/RASS data. A first attempt to clarify the potential of parameterizations in combination with mean profiles from sodar/RASS has recently been made by the campaign Linex-2000 (Engelbart and Steinhagen, 2001).

4. Summary and conclusions

Sodar with(out) RASS, and WPR with(out) RASS, in particular those having operating frequencies around 1 GHz, are becoming more and more standard profiling tools for both monitoring and case studies of the ABL. Apart from mean profiles of wind and temperature, data qualities in particular with respect to higher-order moments like fluxes, still need some improvement, although there are promising results already, as the LITFASS project and the campaign LITFASS-98 had shown.

Concerning the outcomes of the LITFASS project with respect to remote sensing, it has been shown that the determination of ABL height (mixing height) seems to supply reasonable data quality, in particular when combined systems of sodar/RASS and WPR are used. Nevertheless, operational routines still have considerable shortcomings. Higher-order moments, such as variances and fluxes seem to be not yet operational quantities. Concerning WPR, it has nevertheless been shown that this technique is able to supply a good quality of sensible heat fluxes, although its application is restricted yet to some case studies or single vertical profiles. In this respect, the WPR/RASS technique states a cost-effective tool for a supply of validation data for numerical models as requested by the LITFASS project. The current status of data quality after raw-signal processing, i.e., the determination of radial velocities however, does not yet allow to interpret vertical structures in the calculated heat flux profile with respect to surface characteristics usually. Here, promising new possibilities for the future are connected with high-power systems, e.g., 482 MHz WPR/RASS which already have been used for heat flux profiling successfully (Engelbart and Steinhagen, 2001), although this

type of system also shows limitations, which are particularly connected to vertical resolution and minimum height range ($\simeq 500$ m). So in conclusion, the important task remains for sodar systems and particularly those combined with RASS, to supply ABL parameters from the first $300 \cdots 400$ m of height.

References

Angevine WM, Avery SK, Ecklund WL, Carter DA (1993a) Fluxes of heat and momentum measured with a boundary-layer wind profiler radar-radio acoustic sounding system. J Appl Meteor 32: 73–79

Angevine WM, Avery SK, Kok GL (1993b) Virtual heat flux measurements from a boundary-layer profiler/RASS compared to aircraft measurements. J Appl Meteor 32: 1901–1907

Angevine WM, White AB, Avery SK (1994) Boundary-layer depth and entrainment zone characterization with a boundary-layer profiler. Bound-Layer Meteor 68: 375–385

Angevine WM, Bakwin PS, Davis KJ (1998) Wind profiler and RASS measurements compared with measurements from a 450-m-tall tower. J Atmos Oceanic Technol 15: 818–825

Arya SPS (2001) Introduction to micrometeorology. 2nd edn. London: Academic Press, 415 pp

Bange J, Beyrich F, Engelbart DAM (2002) Airborne measurements of turbulent fluxes during LITFASS-98: Comparison with ground measurements and remote sensing in a case study. Theor Appl Climatol (this issue)

Beyrich F (1997) Mixing height estimation from sodar data – a critical discussion. Atmos Environ 31: 3941–3953

Beyrich F, Görsdorf U (1995) Composing the diurnal cycle of mixing height from simultaneous sodar and wind profiler measurements. Bound-Layer Meteor 76: 387–394

Beyrich F, Herzog HJ, Neisser J (2002) The LITFASS project of DWD and the LITFASS-98 experiment: The project strategy and the experimental setup. Theor Appl Climatol (this issue)

Claussen M (1991) Estimation of areally averaged surface fluxes. Bound-Layer Meteor 54: 387–410

Cohn SA, Angevine WM (2000) Boundary-layer height and entrainment zone thickness measured by lidars and wind-profiling radars. J Appl Meteorol 39: 1233–1247

COST-710 (1998) Final report: COST action 710 – Harmonization of the pre-processing of meteorological data for atmospheric dispersion models. vol. EUR 18195 EN. Rue de la Loi 200 (SDME 1/56), B-1049 Brussels, Belgium: ed. B. E. A. Fisher et al., European Commission

Doviak RJ, Zrnic DS (1993) Doppler radar and weather observations – 2nd edn. San Diego, California: Academic Press, 562 pp

Engelbart D (1998) Determination of boundary-layer parameters using Windprofiler/RASS and SODAR/RASS. In: Proceed. 4th Internat. Sympos. on Tropospheric Profiling: Needs and Technologies. Colorado: Snowmass, pp 97–99

Engelbart D, Klein Baltink H (1997) Heat flux measurements by windprofiler/RASS – A comparison with tower data. In: Proc. PWS-97: COST-76 Profiler Workshop, May 12–16, Engelberg, Switzerland, 7–10

Engelbart D, Steinhagen H, Görsdorf U, Lippmann J, Neisser J (1996) A 1290 MHz profiler with RASS for monitoring wind and temperature in the boundary layer. Contrib Atmos Phys 69: 63–80

Engelbart D, Steinhagen H, Görsdorf U, Neisser J, Kirtzel HJ, Peters G (1999) First results of measurements with a newly-designed phased-array sodar with RASS. Meteorol Atmos Phys 71: 61–68

Engelbart DAM, Steinhagen H (2001) The Lindenberg SODAR/RASS experiment LINEX-2000: Concept and first results. In: Meywerk J (ed) Third Study Conference on BALTEX, Mariehamn, Aland, Finland. Publicat. No. 20, Internat BALTEX Secretariat, 55–56

Fay B, Schrodin R, Jacobsen I, Engelbart D (1997) Validation of mixing heights derived from the operational NWP models at the German Weather Service. In: The determination of the mixing height – Current progress and problems, ISBN: 87-550-2325-8. Denmark: Roskilde, pp 55–58

Herzog HJ, Schubert U, Vogel G (2002) LLM – A non-hydrostatic model applied to high-resolving simulations of turbulent fluxes over heterogeneous terrain. Theor Appl Climatol (this issue)

Hirsch L, Peters G (1998) Abilities and limitations of a Radar-RASS wind profiler for the measurement of momentum flux in the planetary boundary layer. Meteor Z 7: 336–344

Lenschow D, Mann J, Kristensen L (1994) How long is long enough when measuring fluxes and other turbulence statistics. J Atmos Oceanic Technol 11: 661–673

Lenschow DH, Stankov BB (1986) Length scales in the convective boundary layer. J Atmos Sci 43: 1198–1209

Müller E, Foken T, Heise E, Majewski D (1995) LITFASS – a nucleus for a BALTEX field experiment. Arbeitsergebn, DWD-GB FE, ISSN 1430-0281, 33: 17 pp

Ottersten H (1969) Atmospheric structure and radar backscattering in clear air. Radio Sci 4: 1179–1193

Peters G, Kirtzel HJ (1994) Measurements of momentum flux in the boundary layer by RASS. J Atmos Oceanic Technol 11: 63–75

Peters G, Hinzpeter H, Baumann G (1985) Measurements of heat flux in the atmospheric boundary layer by sodar and RASS: A first attempt. Radio Sci 20: 1555–1564

Peter G, Fischer B, Kirtzel HJ (1998) One-year operational measurements with a sonic anemomenter–thermometer and a Doppler sodar. J Atmos Oceanic Technol 15: 18–28

Potvin G, MacPherson J, Rogers R, Donaldson N, Strapp J (1998) Analysis of heat flux by RASS and comparison with airplane measurements. Meteor Z: 262–270

Senff C, Bösenberg J, Peters G (1994) Measurements of water-vapor flux profiles in the convective boundary layer with Lidar and Radar-RASS. J Atmos Oceanic Technol 11: 85–93

Soerensen J, Rasmussen A, Svensmark H (1997) Forecast of atmospheric boundary-layer height utilized for ETEX real-time dispersion modeling. Phys Chem Earth 22: 138–146

Steinhagen H, Dibbern J, Engelbart D, Görsdorf U, Lehmann V, Neisser J, Neuschaefer JW (1998) Performance of the first European 482 MHz wind profiler radar with RASS under operational conditions. Meteor Z N F 7: 248–261

Stull RB (1976) The energetics of entrainment across a density interface. J Atmos Sci 33: 1260–1267

Stull RB (1988) An introduction to boundary layer meteorology. Dordrecht, The Netherlands: Kluwer Academic Publisher, 666 pp

Stull RB (1993) Review of non-local mixing in turbulent atmospheres: Transilient turbulence theory. Bound-Layer Meteor 62: 21–96

Vogelezang DHP, Holtslag AAM (1996) Evaluation and model impacts of alternative boundary-layer height formulations. Bound-Layer Meteor 81: 245–269

Weill A (1986) Acoustic remote sensing of the atmosphere and oceans. Atmos Res 20: 103–336

Wulfmeyer V (1999) Investigations of humidity skewness and variance profiles in the convective boundary layer and comparison of the latter with large eddy simulation results. J Atmos Sci: 56: 1077–1087

Wulfmeyer V, Bösenberg J (1998) Ground-based differential absorption lidar for water-vapor profiling: Assessment of accuracy, resolution, and meteorological applications. Appl Opt 37: 3825–3844

Wyngaard JC (1992) Atmospheric turbulence. Rev Fluid Mech 24: 205–233

Authors' addresses: Dr. Dirk A. M. Engelbart (e-mail: Dirk.Engelbart@dwd.de), Deutscher Wetterdienst, Meteorologisches Observatorium Lindenberg, Am Observatorium 12, D-15848 Lindenberg, Germany; J. Bange, Aerospace Systems, Technical University of Braunschweig, Hermann-Blenk-Strasse 23, D-38108 Braunschweig, Germany.